Analytical Imaging Studies Clarifying the Process of the Darkening of Vermilion in Paintings

ARTICLE *in* ANALYTICAL CHEMISTRY · SEPTEMBER 2005

Impact Factor: 5.64 · DOI: 10.1021/ac048158f · Source: PubMed

2 AUTHORS:

Katrien Keune
University of Amsterdam
28 PUBLICATIONS **282** CITATIONS
SEE PROFILE

Jaap J. Boon
JAAP Enterprise for Art Scientific Studies, Am…
332 PUBLICATIONS **8,296** CITATIONS
SEE PROFILE

Anal. Chem. **2005,** *77,* 4742−4750

Analytical Imaging Studies Clarifying the Process of the Darkening of Vermilion in Paintings

Katrien Keune and Jaap J. Boon*

Molecular Paintings Research Group, FOM Institute for Atomic and Molecular Physics, Kruislaan 407, 1098 SJ Amsterdam, The Netherlands

Imaging secondary ion mass spectrometry (SIMS) is applied for the first time to paint cross sections with degraded vermilion (red mercury sulfide) paint to cast new light on the well-known problem of its light-induced darkening. The static SIMS data are combined with light microscopic, electron microscopic studies and energy-dispersive X-ray analysis to identify and localize the various reaction products. The spatial distribution of atomic and molecular species in paint cross sections of the native vermilion and the reaction products leads to the formulation of a new hypothesis on the reaction mechanism of the photodegradation of vermilion where two black and white reaction products are formed sequentially. Under the influence of light, some of the vermilion (HgS) is converted into Hg(0) and S(0). In this process, the chlorine ions, present in the native vermilion, act as a catalyst. We propose that the Hg(0) is deposited on the surface of the remaining HgS as elementary mercury nanoparticles, which turns the vermilion black. Chloride, derived from an external source, is accumulating in the black phase. The metallic mercury and the remaining HgS react away with the excess of chloride. Two intermediate products and a white end product, mercuric chloride ($HgCl_2$), are formed.

Blackening of vermilion (HgS, trigonal), a light-induced degradation phenomenon of HgS, is observed on the raw mineral cinnabar as well as on vermilion paint in works of art. The color change may strongly disfigure the painted image.[1] The highlights in a detail of *Triumphal Procession with Sacrificial Bull* by P. de Grebber (1650) (Oranjezaal, Huis Ten Bosch Palace, The Hague, The Netherlands) should have been vivid red, but are transformed into grayish strokes (Figure 1). This irreversible surface degradation process takes place irrespective of the origin of the vermilion and the type of binding medium.[1] It does not matter whether vermilion has been processed wet or dry or is derived from a natural source as cinnabar.[1] Until recently, the black product on

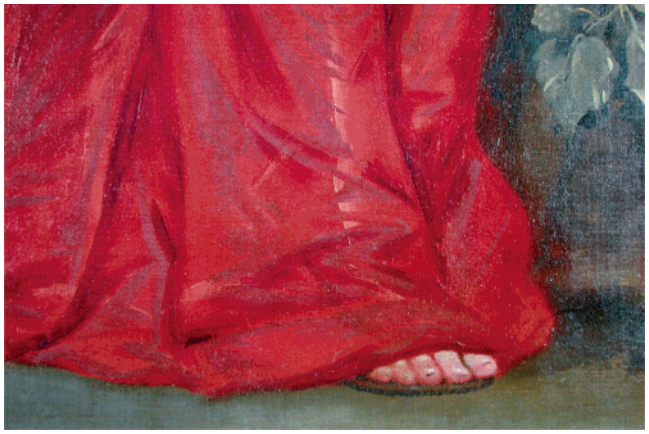

Figure 1. Detail of "Triumphal Procession with Sacrificial Bull" by P. de Grebber (1650) (Oranjezaal, Huis Ten Bosch Palace, The Hague, The Netherlands) showing grayish strokes on top of the red dress. These highlights consist of blackened vermilion. Photo: L. Speleers, Stichting Restauratie Atelier Limburg (SRAL), Maastricht, The Netherlands.

vermilion was thought to be meta-cinnabar (HgS, cubic).[2−5] However, Dreyer already suggested in 1938 that the blackening resulted from a superficial layer of colloidal mercury in solid solution on the cinnabar and that the blacking process was accelerated by impurities.[6] McCormack and others have shown recently that halogen impurities in and around vermilion particles play a dominant role in the darkening process.[4,7,8] Small concentrations of chlorine in cinnabar (average between 0.05 and 1 wt %) can cause blackening, whereas cinnabar with a chlorine concentration less than 0.01 wt % remains unaffected by sunlight.[7] Not only chlorine but also other halogens (mainly iodine) trigger the blackening of vermilion.[4,5,7]

Recently, Spring et al. observed two degradation products in blackened vermilion,[9] a black and white one, which were assumed to be formed simultaneously. It was inferred that vermilion is first transformed into the photosensitive mineral corderoite ($Hg_3S_2Cl_2$) after exposure to humidity and chloride ions. This corderoite

* To whom correspondence should be addressed. E-mail: boon@amolf.nl.

(1) Grout, R.; Burnstock, A. *Z. Kunsttechnol. Konserv.* **2000**, *1*, 15−22.
(2) Feller, R. L. *Studies on the Darkening of Vermilion by Light*, Report and Studies in the History of Art 1967, National Gallery of Art, Washington, DC, 1967.
(3) Gettens, R. J.; Feller, R. L.; Chase, W. T. In *Artist's pigments*; Roy A., Ed.; Oxford University Press: New York, 1993; Vol. 2, pp 167−168.
(4) Daniels, V. In *Recent Advances in the Conservation and Analysis of Artifacts*; Black J., Ed.; Summer School Press: London, 1987; pp 280−282.
(2) Davidson, R. S.; Willsher C. J. *J. Chem. Soc., Dalton Trans.* **1981**, *3*, 833−835.
(3) Dreyer, R. M. *Am. Mineral.* **1938**, *23*, 457−460.
(4) McCormack, J. K. *Miner. Deposita* **2000**, *35*, 796−798.
(5) Davidson, R. S.; Willsher, C. J.; Morrison, C. L. *J. Chem. Soc., Faraday Trans. 1* **1982**, *78*, 1011−1019.
(6) Spring, M.; Grout, R. *Natl. Gallery Technol. Bull.* **2002**, *23*, 50−61.

10.1021/ac048158f CCC: $30.25
Published on Web 06/22/2005

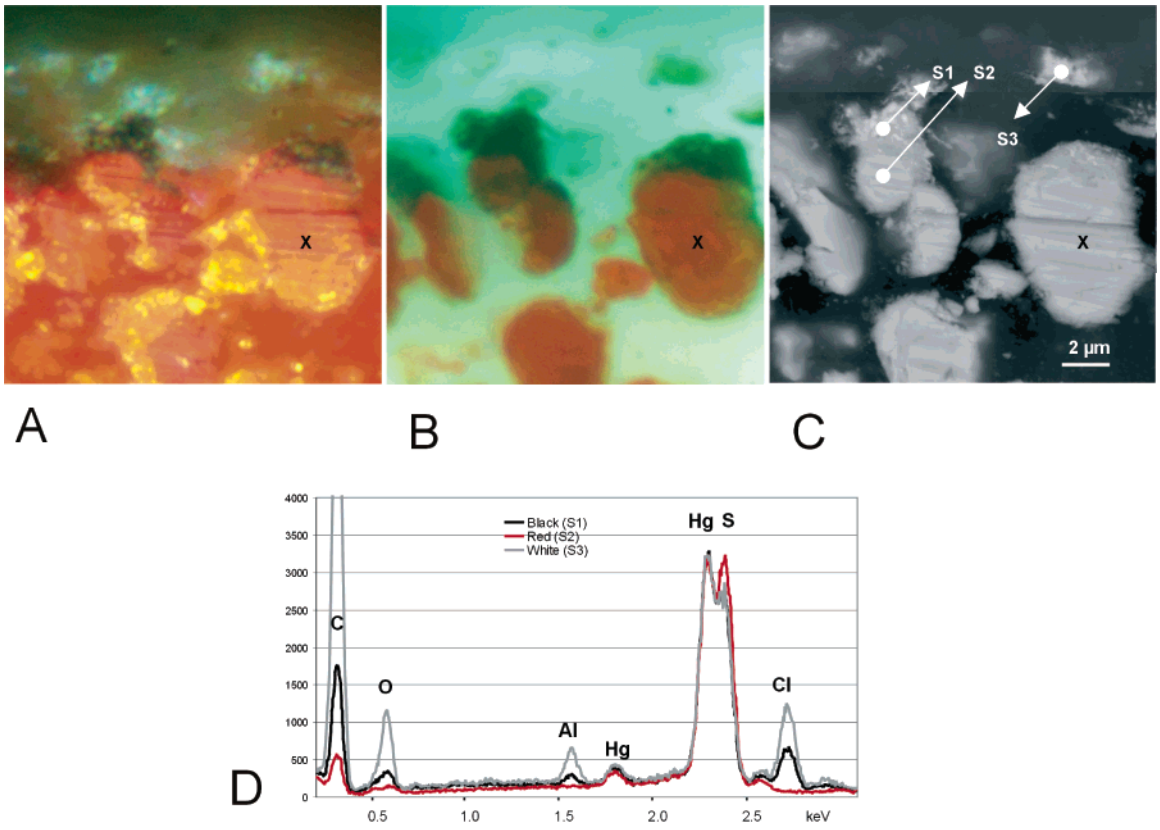

Figure 2. Light microscopic image under white light (A) and UV illumination (B). The image illustrates the partial photodegradation of a vermilion particle. The BSE image (C) shows the structural difference between the red and the black areas. The horizontal lines are due to polishing; the text refers to the particle marked X. EDX spectra of spot analyses (D) in black (S1), red (S2), and white (S3) area demonstrate the different elementary composition of the native material and the reaction products.

subsequently degrades into the black meta-cinnabar, the white calomel (Hg_2Cl_2), and elemental sulfur by a light-induced reaction. The chloride was postulated to originate from external sources.

In general, the degraded vermilion layers in paint cross sections are extremely thin (less than a few micrometers), and most analytical techniques do not have sufficient spatial resolution and sensitivity to study the changes within the paint layer.[4,9] The availability of a paint cross section taken from an (17th century?) overpaint on the painting *Portrait of a Lady* by Peter Paul Rubens (ca. 1625) (Mauritshuis, The Hague; sample number MH251/26) with an extraordinary thick layer of partially degraded, blackened vermilion particles made it possible to investigate the degradation process in more detail (Figures 2A and 3A). In this paper, a second paint cross section from an original layer in *Minerva and Hercules Opening the Doors for Victory* by Christiaan van Couwenberg (1651), (Oranjezaal Huis ten Bosch Palace, The Hague; sample number HSTB 34/2), derived from a collection different from the first sample, is examined as well.

An important advantage of investigating the blackening process of vermilion in paint cross sections is the clear visualization of a gradient in the deterioration from the light-exposed top to the light-shielded bottom. In addition, the pigment particles are embedded in an organic binding medium layer, so the components possibly released during the blackening of vermilion are embedded and fixed in position so they can be investigated by microscopy.

The analytical data obtained from light microscopy, scanning electron microscopy combined with energy-dispersive X-ray analysis (SEM/EDX), and secondary ion mass spectrometry (SIMS) presented here lead to new insights in the mechanism of the blackening of vermilion. In contrast to work presented earlier,[9] we observe that a black reaction product is formed first, which is spatially separated and thus followed by a white compound. We prove that meta-cinnabar cannot be formed, and with the exclusive results from secondary ion mass spectrometry, we could identify another white reaction product that was never before described in paintings.

EXPERIMENTAL SECTION

Samples. The paint sample MH251/26 was embedded in polyester resin Polypol using the Easysection system. Sample HSTB 34/2 was embedded in Technovit 2000LC (Heraeus Kulzer). Both paint cross sections were dry polished with Micromesh polishing cloths (final step 12 000 mesh) (Scientific Instruments Services Inc.).

The following reference materials were used: mercury sulfide (HgS) (Merck), mercuric chloride ($HgCl_2$) (Merck), and mercurous chloride ($(HgCl)_2$) (Fluka).

Instruments. The static SIMS experiments were performed on a Physical Electronics (Eden Prairie, MN) TRIFT-II time-of-flight SIMS. The surface of the sample was scanned with a 15-keV primary ion beam from an $^{115}In^+$ liquid metal ion gun. The pulsed beam was nonbunched with a pulse width of 20 ns, a current of 600 pA, and a spot size of ~120 nm. The primary beam was rastered over a 50 × 50 μm sample area, divided into 256 × 256 pixels. The surface of the sample was charge compensated

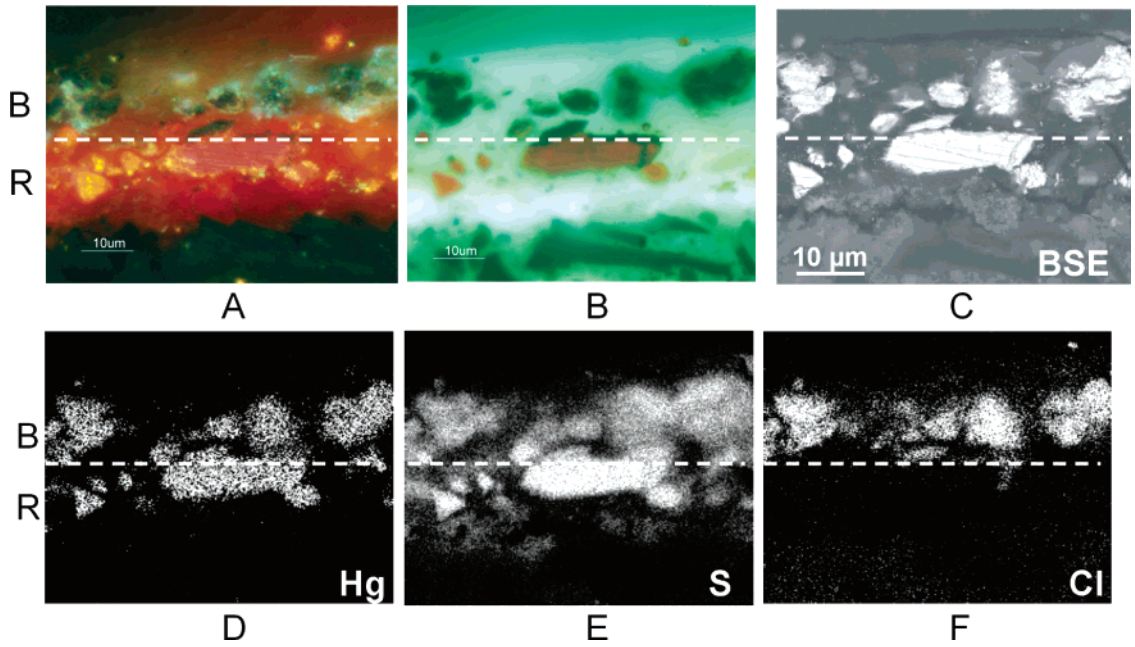

Figure 3. Light microscopic images under white light (A) and UV light (B) illumination and BSE (C) of the partially degraded vermilion paint in paint cross section MH251/26. The images correspond with the area measured with EDX imaging. X-ray maps of intact (R) and blackened (B) vermilion layer reveals the spatial distribution of mercury (Hg L) (D), sulfur (S K) (E), and chlorine (Cl K) (F).

with electrons pulsed between the primary ion beam pulses. To prevent large variations in the extraction field over the large insulation surface area of the paint cross section, a nonmagnetic stainless steel plate with slits (1 mm) was placed on top of the sample. The paint cross section (150 × 50 × 3 mm) was rinsed in hexane to eliminate contamination of airborne silicones.

A 15-keV $^{115}In^+$ primary ion beam was used for the reference samples, with primary ion pulses that were compressed (bunched) to ~1 ns to obtain a better mass resolution. These experiments were performed with 600 pA beam current. All these measurements were charge compensated with electrons pulsed between the primary ion beam pulses.

The oil immersion reflected light microscopic images were obtained on a Leica DMRX microscope (Leica, Wetzlar, Germany). White light was provided by a 100-W halogen lamp, and an Osram HBO 50-W lamp and Leica filter D (excitation 360−425 nm, emission >460 nm) were used for fluorescence microscopy. The surface of the paint cross section was covered with immersion oil (Catalog No. 11 513 787, Leica). Images were recorded with a Nikon digital still camera DXM1200 (Nikon Instech Co., Ltd.).

Scanning electron microscopy studies in combination with energy-dispersive X-ray analysis were performed on a XL30 SFEG high-vacuum electron microscope (FEI, Eindhoven, The Netherlands) with EDX system (spot analysis and elemental mapping facilities) from EDAX (Tilburg, The Netherlands). Backscattered electron images of the cross sections were taken at 20-kV accelerating voltage at a 5-mm eucentric working distance and a spot size of 3, which corresponds to a beam diameter of 2.2 nm with current density of ~130 pA. EDX analysis was performed at a spot size setting of 4 (beam diameter 2.5 nm and current density 550 pA) to obtain a higher count rate and at an acceleration voltage of 20 kV. EDX mapping parameters were as follows: 256 × 200 matrix, 1028 frames, 100-μs dwell time, and 50-μs amplitude time. Samples were carbon coated to improve surface conduction in a CC7650 Polaron Carbon Coater with carbon fiber (Quorum Technologies, East Sussex, U.K.).

RESULTS

Light Microscopy. Light microscopic images of a highly magnified area of discolored vermilion in the paint cross section MH251/26 are shown in Figures 2A, 3A, and 4A (normal light) and 2B and 3B (UV light). The area of the panel painting of the sample MH251/26 is overpainted, and the paint buildup consists now of at least six layers. The original paint layers consist of a chalk ground, a lead white, and charcoal imprimatura and finally several layers of vermilion and red lake. A bone black layer blocks out this original red paint. On top, a thin organic intermediate layer is applied with as final layer the now degraded vermilion with red lake (paint cross section not shown). The total thickness of the vermilion layer is 25 μm of which 15 μm is discolored, containing both the black and white degradation products. The vermilion particles are coarse grained, and the individual particles are partially degraded in some instances. These latter particles consist of a black upper part and a red lower part (in UV light, the colors remain black and red). The white product is positioned on top and around the black product and is transparent under UV illumination.

A magnified area of the darkened vermilion in paint cross section HSTB 34/2 is shown in Figure 5A and B (normal and UV light). There are three layers in the area of the panel painting where the sample was removed: a grayish lead white ground, a reddish-brown iron oxide paint layer, and a red paint layer with a mixture of vermilion and red lake on top (paint cross section not shown). The degraded top layer with black and white products is very thin (4 μm), while the total thickness of the vermilion and red lake layer is 50 μm. The intact layer consists mainly of finely dispersed vermilion particles with a few larger ones. Red lake is

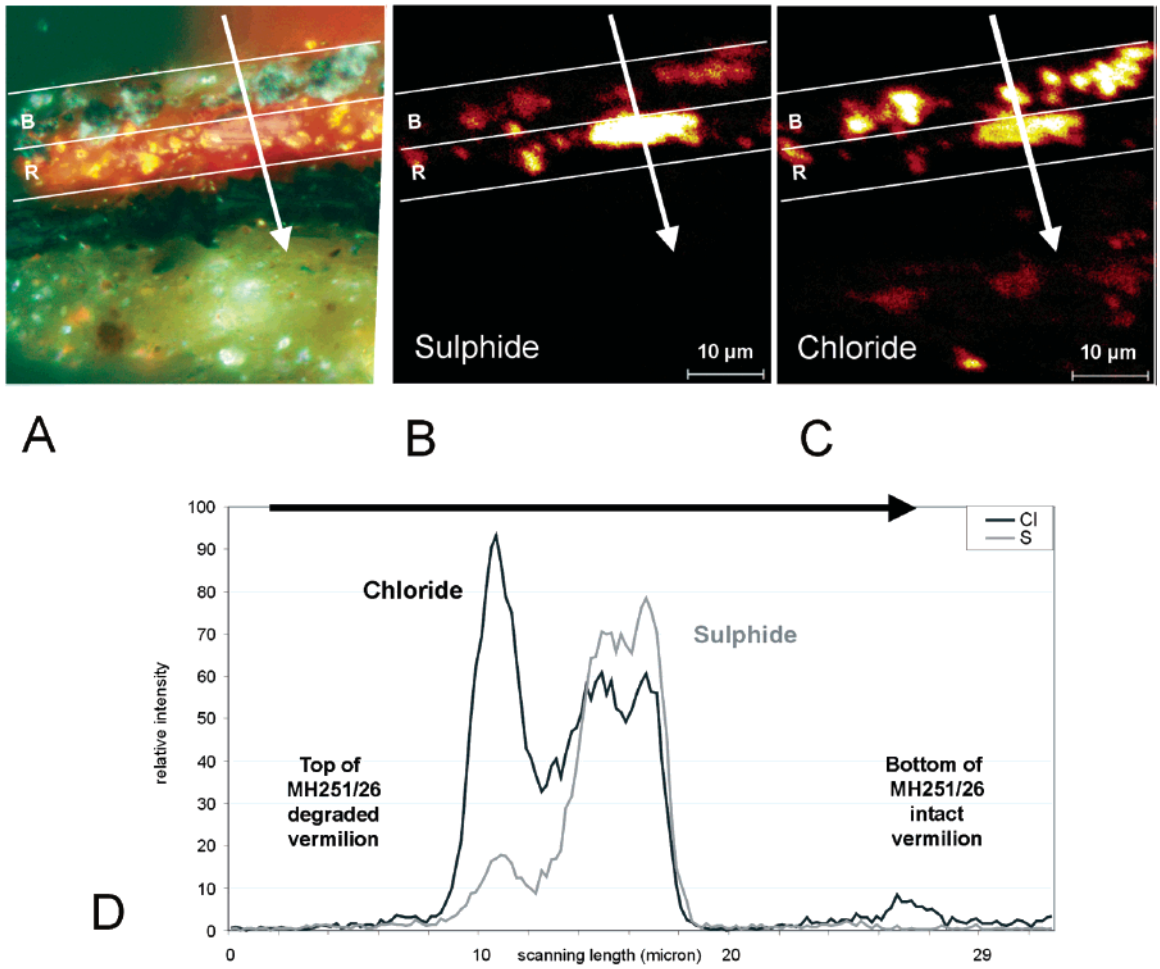

Figure 4. Light microscopic image (A), representing the scanned SIMS area of the partially degraded vermilion paint of MH251/26. The arrow indicates the direction of the line scan. SIMS images of the sulfide (B) and chloride (C) represent the distribution of these ions over the partially degraded vermilion paint layer. The line scan (D) illustrates the distribution of chlorine and sulfur from top to bottom in the paint cross section.

present in the vermilion layer and is recognizable by the pinkish fluoresce in the UV image (Figure 5B).

SEM/EDX. The backscattered electron image (BSE-image) illustrates the presence of a structural change in the partially degraded vermilion particle of MH251/26 (Figure 2C). The structure of the red vermilion particle differs from the structure of the black product. The red part of particle X (indicated in Figure 2C) is flat and homogeneous. The horizontal lines in the particles are polishing marks. The black part of the particle X is irregular and broken up. Spots with a higher BSE intensity and a size smaller than 100 nm are visible in the degraded black phase (Figure 2C and Supporting Information Figure 1). The white areas display the same BSE intensity as the black and the red areas.

The two elements in vermilion—mercury and sulfur—are detected with EDX spot analysis in the red (S2), black (S1), and white (S3) particles (Figure 2D). EDX spot analyses of the red (S2), black (S1), and the white (S3) phases demonstrate that there is relatively less sulfur in the degraded particles (Figure 2D), considering the sulfur/mercury ratio. This sulfur/mercury ratio is only indicative because the X-ray intensity peaks of the mercury M-shell and the sulfur K-shell are partially overlapping. EDX spot analysis from the black area (S1) and white area (S3) shows relatively high chlorine counts; the chlorine concentration in the white particle is much higher than in the black particle (taking the mercury peak as reference). The EDX spectrum of the white area reveals that the intensities of carbon, oxygen, and aluminum are high compared to the black and red areas. However, these elements are representative for the organic binding medium and are only detected due to the fact that the interaction volume of the beam is larger than the volume of the particle. The sulfur-to-mercury ratio in the binding medium of both the degraded and intact parts is higher than the red particles (spectrum not shown), which indicates that sulfur, besides being a constituent of HgS, is also present in another form in the binding medium.

Elemental X-ray maps of the affected vermilion layer in MH251/26 visualize the distribution of mercury, sulfur, and chlorine (Figure 3). The dotted line in the elemental images indicates the compositional transition between red (R) and black (B) particles (Figure 3). The elemental X-ray map of mercury illustrates that mercury is only present inside the pigment particles and has not diffused into the binding medium. Sulfur is present in high relative intensity in the mercury containing particles of the intact layer (R), whereas lower sulfur X-ray counts are observed in and around the degraded particles (B). The chlorine is only detected in high counts in the degraded vermilion particles.

SIMS. SIMS spectra were acquired in the negative ion mode. Chloride and sulfide dominate in the SIMS spectra of MH251/26 and HSTB 34/2. The spatial distribution of the sulfide and chloride

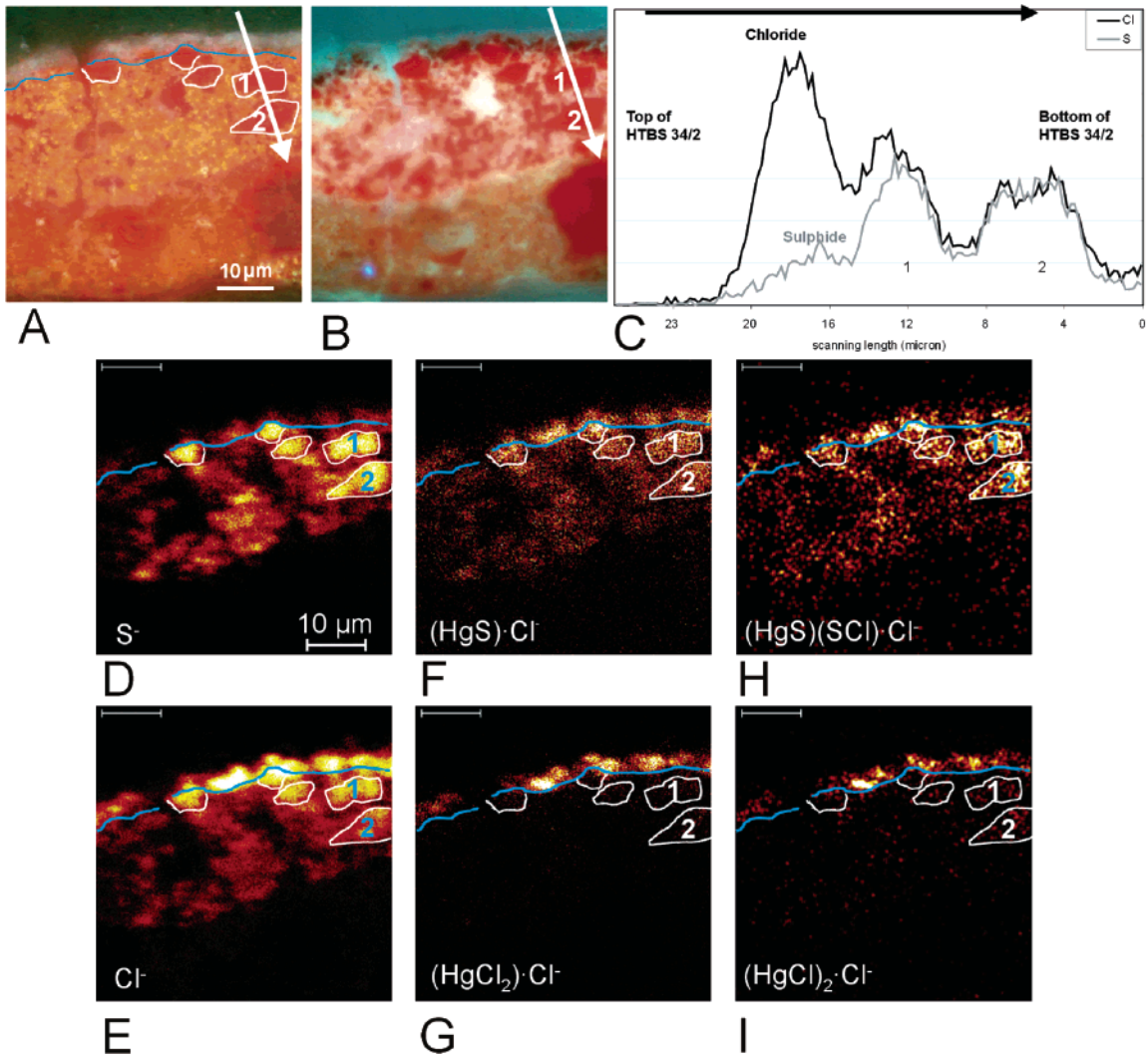

Figure 5. Distribution of sulfide and chloride and the molecular distribution in a partially degraded vermilion paint. The arrow in the light microscopic image (A) and UV light image (B), which represents the scanned SIMS area, indicates the direction of the line scan (C). The negative SIMS image of mercury−halogen cluster ions elucidates the position of S^- (D), Cl^- (E), $(HgS)Cl^-$ (F), $(HgCl_2)Cl^-$ (G), $(HgS)(SCl)Cl^-$ (H), and $(HgCl)_2Cl^-$ (I) in the partially degraded vermilion paint. A contour, based on the light microscopic image and total negative ion image, outlines four red vermilion particles and the boundary between the intact and degraded paint.

ions in sample MH251/26 is plotted in Figure 4B and 4C, respectively. Figure 4A represents the light microscopic image of the scanned SIMS area. Three horizontal lines in the images in Figure 4 outline the blackened layer (B) and the red vermilion layer (R). The intact red vermilion particles contain sulfide and chloride (see layer R in Figure 4B and C). The chloride is present in higher amounts in the degraded layer (B) and corresponds to the black and white particles. Line scans drawn from the top to the bottom of the layer (see white arrows in Figure 4A−C) visualize the distribution of the secondary ion yields. The secondary ion yields of both chloride and sulfide ions are depicted in Figure 4D. The line scan, with a resolution of 1 μm, first crosses a degraded vermilion particle (3 μm) and then scans an intact vermilion particle (5 μm). The chloride ion yield is higher for degraded vermilion compared to the intact vermilion. The sulfide ion yield is relatively diminished in the degraded particles compared to the intact vermilion. The same phenomenon is observed in paint cross section HSTB 34/2 (Figure 5C). The line scan crosses the degraded vermilion layer (4 μm) and two intact vermilion particles (6 μm) (Figure 5A−C). The chloride and sulfide ion distribution are displayed in Figure 5D and E.

Similar negatively charged mercury−halogen cluster ion patterns were detected in the paint cross sections MH251/26 and HSTB34/2. The corresponding molecules were deduced on the basis of their molecular weight distribution and isotopic pattern. The SIMS spectra of HSTB 34/2 show the cluster ions from $[Hg_nS_nCl]^-$ ($n = 1-6$), $[Hg_nS_{n-1}Cl_3]^-$ ($n = 1-4$), and $[Hg_nS_{n+1}Cl_2]^-$ ($n = 1-3$). The spectra of sample MH251/26 show the same types of cluster ions, but only for $n = 1-2$ (full spectra not shown; a partial negative ion spectrum of HSTB 34/2 with $n = 3$ is discussed in the next paragraph). The ions are interpreted as chloride adduct ions from $(HgS)_n$ $[(HgS)_n \cdot Cl^-$ ($n = 1-6$)], $(HgS)_n(HgCl_2)$ $[(HgS)_n(HgCl_2) \cdot Cl^-$ ($n = 0-3$)], and $(HgS)_n(SCl)$ $[(HgS)_n(SCl) \cdot Cl^-$ ($n = 1-3$)], respectively. Other types of cluster ions detected with lower ion yields in the paint sample are $(HgCl)_2 \cdot Cl^-$ and $Hg_nS_yCl^-$ ($y = n + 1$, $n + 2$, or $n + 3$). $(HgS)_n \cdot Cl^-$, $(HgS)_n(SCl) \cdot Cl^-$, and $Hg_nS_yCl^-$ are detected in the intact and degraded vermilion particles of HSTB 34/2, whereas $(HgS)_n$(Hg-

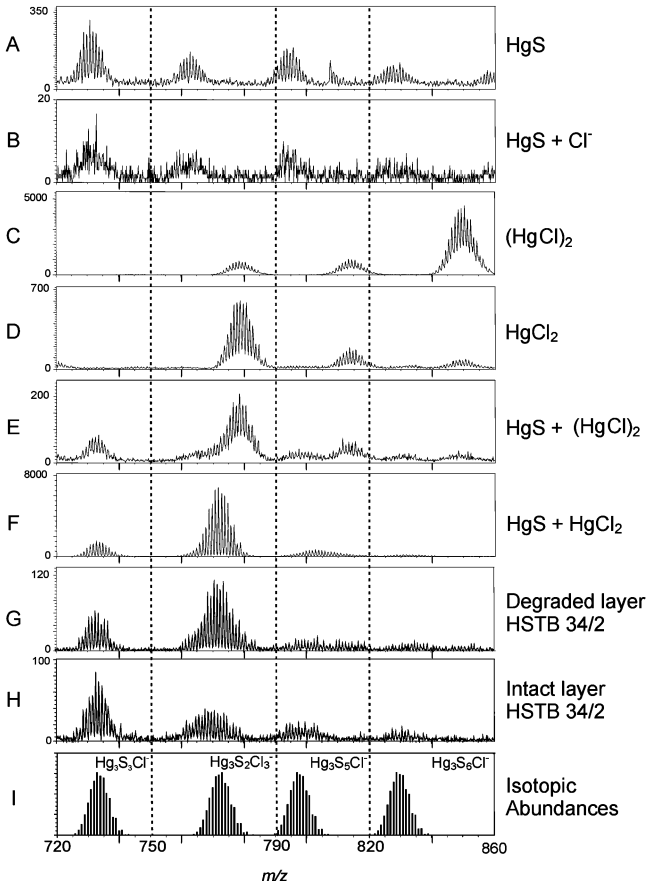

Figure 6. Part of the negative ion mass spectrum in the mass range 720−860 amu of pure HgS (A), HgS + Cl^- ions (B), pure $(HgCl)_2$ (C), pure $HgCl_2$ (D) mixture of HgS + $(HgCl)_2$ (E), mixture of HgS + $HgCl_2$ (F), degraded vermilion layer in paint cross section HSTB 34/2 (G), intact vermilion layer in paint cross section HSTB 34/2 (H), and calculated isotopic distribution of $(Hg_3S_3)Cl^-$, $(Hg_3S_2Cl_2)Cl^-$, $(Hg_3S_5)Cl^-$, and $(Hg_3S_6)Cl^-$ (I). The vertical dotted lines divide the spectra into four mass ranges, which correspond with the columns in Table 1.

$Cl_2)\cdot Cl^-$ and $(HgCl)_2\cdot Cl^-$ are only detected in the degraded layer. The SIMS images in Figure 5F−I illustrate this distribution of $(HgS)\cdot Cl^-$, $(HgCl_2)\cdot Cl^-$, $(HgS)(SCl)\cdot Cl^-$, and $(HgCl)_2\cdot Cl^-$ in HSTB 34/2. A contour drawn on the basis of the light microscopic image and the total negative ion image outlines five red vermilion particles and the boundary in blue between the intact and degraded paint.

Figure 6A−F represents partial negative ion mass spectra of the reference materials HgS, $(HgCl)_2$, and $HgCl_2$ and their mixtures HgS + $(HgCl)_2$ and HgS + $HgCl_2$. The reference materials, $HgCl_2$ and $(HgCl)_2$, are two separate white mercury chloride complexes that are suspected to be present in the degraded vermilion layer of paint cross section HSTB 34/2. Part of the negative ion mass spectrum of the degraded vermilion paint in paint cross section HSTB 34/2 is depicted in Figure 6G. The spectrum is acquired after selecting the region of interest in the total area analyzed (50 μm^2). The SIMS spectrum of the intact vermilion is represented by Figure 6H. Figure 6I represents the calculated isotopic distributions of the ion clusters $(Hg_3S_3)Cl^-$, $(Hg_3S_2Cl_2)Cl^-$, $(Hg_3S_5)Cl^-$, and $(Hg_3S_6)Cl^-$. These ions were chosen for calculation because they match the mass window of the relevant cluster ion peak patterns from mercury−halogen cluster ions with three mercury atoms in the regions of interest.

Table 1. Overview of the Various Mercury−Halogen Cluster Ions Detected in the Negative Ion Mass Spectra in the Mass Range of 720−860 Amu Originating from the Reference Materials, Their Mixtures, and the Degraded and Intact Vermilion Layer in HSTB 34/2

	mass range,[a] amu			
sample	720−750	750−790	790−820	820−860
HgS	$(HgS)_3S^-$	$Hg_3S_5^-$	$Hg_3S_6^-$	$Hg_3S_7^-$
HgS + Cl^-			$Hg_3S_6^-$	
$HgCl_2$		$(Hg_3Cl_4)Cl^-$	$(Hg_3Cl_5)Cl^-$	$(Hg_3Cl_6)Cl^-$
Hg_2Cl_2		$(Hg_3Cl_4)Cl^-$	$(Hg_3Cl_5)Cl^-$	$(Hg_3Cl_6)Cl^-$
HgS + $HgCl_2$	$(HgS)_3Cl^-$	$(Hg_3S_2Cl_2)Cl^-$	$(Hg_3S_2Cl_3)Cl^-$ $(Hg_3S_3Cl_2)Cl^-$ $(Hg_3S_4Cl)Cl^-$	$(Hg_3S_6)Cl^-$
HgS + Hg_2Cl_2	$(HgS)_3Cl^-$	$(Hg_3Cl_4)Cl^-$	$(Hg_3Cl_5)Cl^-$	$(Hg_3Cl_6)Cl^-$
degraded layer HSTB-34/2	$(HgS)_3Cl^-$	$(Hg_3S_2Cl_2)Cl^-$ $(Hg_3S_4)Cl^-$ $(Hg_3SCl_3)Cl^-$		
intact layer HSTB 34/2	$(HgS)_3Cl^-$	$(Hg_3S_2Cl_2)Cl^-$ $(Hg_3S_4)Cl^-$	$(Hg_3S_5)Cl^-$	$(Hg_3S_6)Cl^-$

[a] The four mass ranges correspond to the mass ranges indicated in Figure 6.

The SIMS spectra of the reference materials and their mixtures support the identification of the new products present in the degraded vermilion paint layer of HSTB 34/2. Vertical dotted lines pasted over the mass spectra in Figure 6 divide these into four mass windows corresponding to the four columns in the Table 1. Table 1 gives an overview of the interpreted mercury−halogen cluster ion patterns in four mass windows deduced from the spectra of the various reference materials and the paint cross section present (Figure 6 and Table 1).

In the mass window from 720 to 750 amu, $(HgS)_3Cl^-$ (m/z 726−743) is detected in the mass spectrum of intact and degraded vermilion in HSTB 34/2 (Figure 6G and H). The reference spectra of both mixtures (HgS + $HgCl_2$ and HgS + $(HgCl)_2$) show the same cluster ions (Figure 6E, F), while the spectrum of pure HgS shows a $(HgS)_3S^-$ cluster ion without a chloride ion attached (Figure 6A). In the mass window from 750 to 790 amu, peaks at 760−781 amu assigned to $(Hg_3S_2Cl_2)Cl^-$ are dominant in the mass spectrum of the degraded vermilion (Figure 6G). The ion cluster $(Hg_3S_2Cl_2)Cl^-$ is only found in the spectrum of the mixture of HgS + $HgCl_2$ (Figure 6F). A relative small amount of $(Hg_3S_4)Cl^-$ and $(Hg_3SCl_3)Cl^-$ in this mass range is detected in the degraded vermilion (these cluster ions partially overlap with the cluster ions of $(Hg_3S_2Cl_2)Cl^-$). In the intact vermilion, relatively minor contributions from $(Hg_3S_2Cl_2)Cl^-$ and $(Hg_3S_4)Cl^-$ are detected (Figure 6H). The mass window from 790 to 820 amu shows $(Hg_3S_5)Cl^-$ and $(Hg_3S_4Cl)Cl^-$ in the mass spectrum of the intact vermilion of HSTB 34/2. The latter cluster ion is found in low yields in the spectrum of the mixture [HgS + $HgCl_2$]. In the mass window from 820 to 860 amu, the cluster $(Hg_3S_6)Cl^-$ is detected in low yields in spectra of the paint cross section as well as in the mixture HgS + $HgCl_2$ (Figure 6F and H and Table 1).

Figure 6B represents the SIMS spectrum of the reference material HgS with an excess of chloride ions added as KCl. We conclude that the mercury−halogen cluster ions detected in the paint cross section are not formed by gas-phase ion chemistry just above the surface after SIMS of HgS and KCl, because

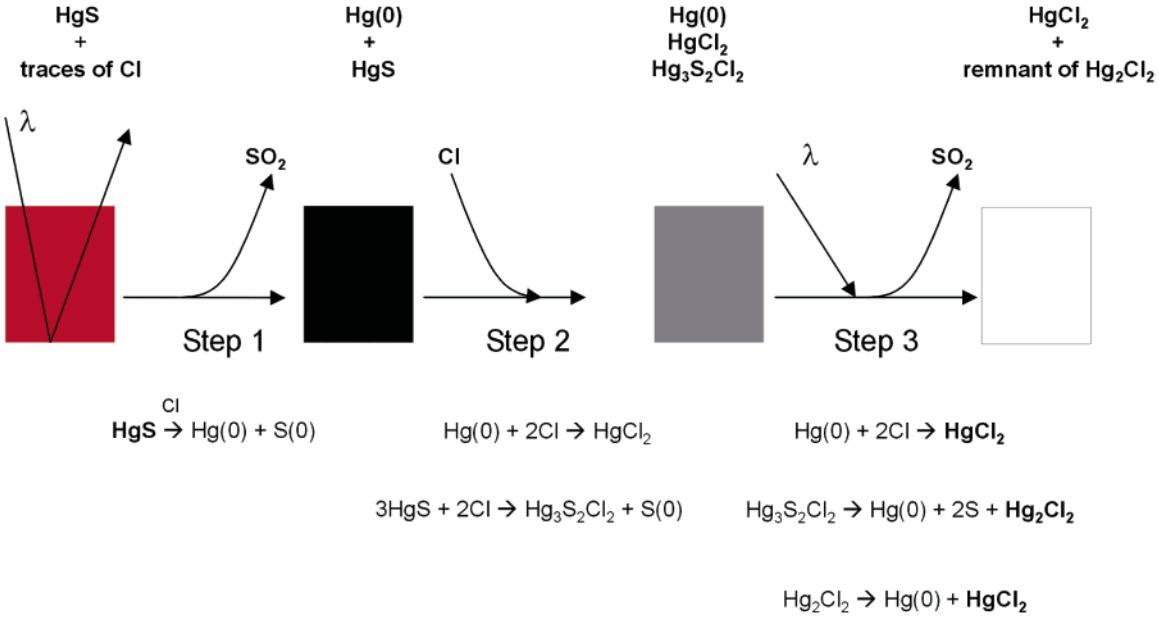

Figure 7. Scheme of the proposed mechanisms of the degradation process of the red vermilion into a black and finally a white product.

$(HgS)_n(HgCl_2)\cdot Cl^-$ and $(HgCl)_2\cdot Cl^-$ are not observed in this spectrum. The exact identification of the composition of the mercury−halogen cluster ions in Figure 6B is difficult as the yields and thus the resolution is low.

DISCUSSION

The two paint cross sections investigated that originate from paintings made by two different painters and that were kept under different conditions give similar analytical information on the color changes in vermilion. The analytical imaging studies on the darkened vermilion oil paint layer in sample MH251/26 demonstrate the degradation phenomena in detail. As light is a requirement for the degradation process, it is concluded that the light must have penetrated the whole affected layer as all particles in sample MH251/26 are homogeneously transformed. On the basis of the transition of the red into the black materials observed in the partially degraded particles and the position of the white materials around the black materials, we propose that the black material is formed first. In a later stage, the white product is formed from the black reaction product.

Both the SIMS and EDX techniques show relatively high amounts of chloride and relatively low amounts of sulfide in the degraded particles. The relative amount of mercury in the intact and degraded particles is considered to be constant, since the backscattered electron intensity in the BSE image is the same for all phases. The EDX images lead us to conclude that sulfur leaches from the particles in the degraded layer into the environment. However, EDX spot analyses detect sulfur in the organic binding medium of both the degraded and the intact part. The organic binding medium also has been shown to contain aluminum. Sulfur and aluminum are known constituents of the inorganic substrate of red lakes.[10] It is therefore possible that red lake has been mixed into the paint although no distinct pigment particles are visible.

The mercury−halogen cluster anions detected in the whole vermilion layer with SIMS are charged by attachment of Cl^- ions. Neutral molecules are known to be anionized by chloride to form a negatively charged complex.[11,12] The ions $(HgS)_nCl^-$ and $(HgS)_n(SCl)Cl^-$ are found in the intact vermilion paint layer and are representative for intact HgS. $(HgS)_nS^-$, detected in the pure HgS, is not present in the SIMS spectra of the mixtures and may be suppressed by the presence of chloride. Ions from $(HgS)_n(HgCl_2)\cdot Cl^-$ ($n = 0-6$) are detected and mainly present in the degraded vermilion layer. These types of ions are also formed from the mixture of HgS + $HgCl_2$ but not from the mixture HgS + $(HgCl)_2$. We conclude on the basis of the presence of these types of ions found in the degraded vermilion layer that it is indicative for mercuric chloride ($HgCl_2$). In addition, the ions from $(HgS)_n(HgCl_2)\cdot Cl^-$ detected in SIMS data of a mixture of HgS + $HgCl_2$ indicate that HgS is still present in the degraded vermilion layer, because these ions are absent in the spectra of pure $HgCl_2$. The ions $(HgCl)_2\cdot Cl^-$ are not only representative for $(HgCl)_2$ (calomel), because these ions are also detected in the spectrum of HgS + $HgCl_2$ (part of the spectrum not shown). It is concluded that the presence of calomel in the paint sample cannot be proven with SIMS, because this ion $(HgCl)_2\cdot Cl^-$ is not characteristic for $(HgCl)_2$ (calomel) and $(Hg_3Cl_4)\cdot Cl^-$ is only detected in the HgS + $(HgCl)_2$ reference mixture and not in the paint sample.

On the basis of our results and literature data, we propose that the transformation of vermilion from red into black materials is a conversion from HgS into Hg(0) and S(0) by a photochemical reaction catalyzed by chloride (step 1 in Figure 7). The conversion of Hg(0) from photoreduced Hg(II) has been reported both in solid phase[13] and aqueous media.[14−19] This supports the idea of

(10) Schweppe, H.; Winter, J. In *Artist's pigments*; West FitzHugh, E. Ed.; Oxford University Press: New York, 1997; Vol. 3, Chapter 4.

(11) Groenewold, G. S.; Appelhaus, A. D.; Gresham, G. L.; Ingram, J. C.; Shaw, A. D. *Int. J. Mass Spectrom.* **1998**, *178*, 19−29.

(12) Delcorte, A. In *ToF-SIMS: Surface Analysis by Mass Spectrometry*' Vickerman, J. C., Briggs, D., Eds.; IM Publication and Surface Spectra Limited: London, 2001; p 183.

(13) Gustin, M. S.; Biester, H.; Kim, C. S.; *Atmos. Environ.* **2002**, *36*, 3241−3254.

the light-induced conversion of Hg(II)S into Hg(0). After the photoreduction reaction, the metallic mercury is deposited on the intact HgS surface, resulting in a black reaction product. The remaining HgS in the degraded vermilion is identified with SIMS. The metallic mercury is present as nanoparticles, which is supported by the "hot" spots smaller than 100 nm visualized in the BSE-image (Figure 2C and Supporting Information, Figure 1). The Hg(0) precipitation on the vermilion surface has never been proven directly, but has been suggested by other authors.[6,16,20] Elementary sulfur is also detected as a product of photodegraded HgS.[19] The sulfur leaves the paint particles possibly in the form of volatile sulfur oxide, as sulfur has been shown to oxidize to sulfate ions via polythionic acids.[21] Since the sulfur is lost from the particle, it is inferred that a conversion of vermilion to meta-cinnabar is unlikely. The small relative concentration of sulfur still present in the particles is ascribed to intact residual intact vermilion. XRD measurements performed on reconstructions and other paint samples elsewhere by other authors support this conclusion.[1,2,4,7,9] It is shown that vermilion is still present in the XRD spectra of the blackened vermilion as is deduced from the decreased intensity of the XRD patterns of vermilion. No black meta-cinnabar was shown in the XRD spectra.

Chlorine plays a dominant role in the light-induced blackening phenomenon, as already suggested in the literature.[7,9] The much more sensitive surface technique of SIMS demonstrates, in contrast to the EDX results, that chloride is present inside the vermilion particles of both MH 251/26 and HSTB 34/2. The concentration of chloride in the red particles must be below the detection limit of EDX. As small quantities of chloride make vermilion photosensitive,[7] the small amounts of chloride detected in the intact vermilion trigger the blackening process. Due to the fact that only small quantities of chloride are necessary to form blackened cinnabar and that other compounds besides chloride ions, such as iodide, enhance the blackening as well, it is concluded that chloride initially acts as a catalyst and is not part of the primary reaction products. The exact minimum concentration of chloride necessary to trigger the process is not known. McCormack states that cinnabar is light stable below 0.01 wt % (±0.01 wt %) chloride, as determined with a wavelength-dispersive microprobe analyzer cinnabar is light stable and it blackens at a concentration of 0.05 wt % and higher.[7]

The exact mechanism of the photodegradation of vermilion catalyzed by chloride is still an open question. We suggest that under the influence of light an electron−hole pair is generated and a photoeletrochemical process takes place, which enables an electron transfer from chlorine anion to mercury and from sulfide back to chloride (i.e., chloride has a catalytic function). Assuming that chlorine anions are oxidized by the positive holes of the valence band of HgS, the valence band edge of HgS must be more positive than the redox potential of Cl^-/Cl_2.[16,22] The exact position of the valence band edge of HgS is not clear, but the value of this position is expected to be close to the redox potential of Cl^-/Cl_2.[22]

The relatively high quantity of chloride in the degraded part is hard to explain from an original vermilion source alone. We also have to conclude that the chloride is not introduced via the binding medium, as EDX did not detect chloride in the binding medium of the intact area. To explain the relatively high yields of chloride ions in the degraded vermilion particles, it is necessary to invoke additional source of chlorides. Chloride is possibly transported by diffusion from paint layers positioned lower or introduced from an external source.

After the first transformation, the black product is thought to trap chloride to transform subsequently into a white reaction product. Although the elemental composition (Hg, S, Cl) of the black and the white phases is the same, the EDX spot analysis shows a higher relative intensity of chlorine and a fairly lower relative intensity of sulfur in the white product (S3) compared to the black product (S1) (Figure 2A and D). SIMS identifies the mercury chlorine complex $HgCl_2$ in the degraded vermilion layer. Mercuric chloride ($HgCl_2$) has never been identified in paintings before. Calomel $(HgCl)_2$ cannot be identified positively with SIMS; however, Spring and Grout had identified calomel as the white product in paintings containing degraded vermilion using Raman microscopy.[9]

The two components in the black product, metallic mercury and residual vermilion, react with chloride supplied by sources external to the vermilion. The residual vermilion reacts with this external chloride to the light-sensitive mineral corderoite, which degrades under the influence of light into calomel, metallic mercury, and sulfur. Corderoite ($Hg_3S_2Cl_2$) can easily be formed in a mixture of HgS and NaCl solution kept at room temperature after a long period[7,9] and will after light exposure degrade into a dark gray product containing $(HgCl)_2$.[9] The formation of corderoite could not have taken place in the first degradation steps, because of the high amount of chloride required that is suggested to accumulate after the blackening. The $(HgCl)_2$ formed photodegrades under normal light into $HgCl_2$ and Hg(0).[23] The metallic mercury, derived from the photoreduction in the first step, the corderoite, and the $(HgCl)_2$, react with chloride to form mercuric chloride $HgCl_2$. In vitro, $HgCl_2$ can be formed from metallic mercury via the reaction with chlorine gas or by the formation of mercury(II) sulfate.[24] The white end product is found around the black product, which means that external sources, light, and a higher concentration of chloride are necessary to create the white product.

Figure 7 illustrates the scheme of the proposed mechanisms of the degradation process of the red vermilion into the black and subsequently the white reaction product. The scheme describes the degradation phenomena qualitatively to clarify the process. The products observed in the paint cross sections are mixed phases and consequently cannot be classified in a single

(14) Hsieh, Y. H.; Tokunaga, S.; Huang, C. P. *Colloids Surf.* **1991**, *53*, 257−274.
(15) Ravichandran, M. *Chemosphere* **2004**, *55*, 319−331.
(16) Pal, B.; Ikeda, S.; Ohtani, B. *Inorg. Chem.* **2003**, *42*, 1518−1524.
(17) Litter, M. I. *App. Catal., B* **1999**, *23*, 89−114.
(18) Strömberg, D.; Strömberg, A.; Wahlgren, U. *Water, Air, Soil Pollut.* **1991**, *56*, 681−695.
(19) Okouchi, S.; Sasaki, S. *Environ. Int.* **1983**, *9*, 103−106.
(20) Gaustin, M. S.; Maxy, R. A.; Rasmussen, P. In *Symposium Volume of Air Pollutance*, Cary, NC, September 1998.
(21) Naito, K.; Takei, S.; Okabe, T. *Bull. Chem. Soc. Jpn.* **1970**, *43*, 1360−1364.
(22) Personal communication with Professor B. Ohtani (Catalysis Research Center, Hokkaido University, Japan), 2004.
(23) Chambers, C.; Holliday, A. K. In *Modern Inorganic Chemistry*; Butterworth & Co.: London, 1975; p 437.
(24) Holleman, A. F.; Wilberg, E. In *Inorganic Chemistry*; Academic Press: San Diego, 2001; p 1310.

category in the scheme. For example, the black product in sample MH251/26 has a relatively higher concentration of chloride compared to the intact red vermilion. Based on its color, this black product would be classified in the black box after step 1 in the diagram, but a relative increase in chloride is taking place. This accumulation in the black product is indicated in step 2, but a conversion into a white product is not observed with light microscopy. Therefore, the black product would be classified in the box after step 2, which is indicated in the scheme as gray. Furthermore, not all the degraded vermilion is converted into $HgCl_2$ in sample HSTB 34/2; some of the former reaction products are still expected to be present.

The obtained knowledge implies that the quality of the vermilion used in paintings is of significant importance for the changes of preservation of the red color. Small chloride or other halogen impurities in the vermilion makes the red pigment photosensitive. Chloride present in the medium or derived from other external sources can drive subsequent reactions. Works of art such as easel and mural paintings can be expected to be exposed to light and chlorides.

CONCLUSION

Analytical studies on paint cross sections containing darkened vermilion reveal the light-induced degradation phenomena in detail. Light microscopic images reveal two colored reaction products, a white product positioned above and around a black product. SEM/EDX data give information about the elemental distribution and the structural changes between the three colored phases. SIMS detects, in contrast to EDX, traces of chloride in the native vermilion. The additional benefit of imaging SIMS applied for the first time to investigate this phenomenon in paint cross sections is that the molecular information from SIMS is able to identify the white reaction product as mercuric chloride. We propose a new hypothesis, which describes a three-step process where black and white reaction products are formed from each other. Chloride acts as catalyst in the first step of the photoinduced chemical degradation of vermilion. In the formed black reaction product, an excess of chloride is accumulated. The black phase will react further with the excess of chloride to form the white product, mercuric chloride. The combination of both techniques, SEM/EDX and SIMS, is essential to elucidate the familiar phenomenon of "blackening of vermilion" in detail.

ACKNOWLEDGMENT

We are grateful to Linnaea Saunders, Mauritshuis, The Hague, The Netherlands, who provided us the paint cross section MH251/26. We also thank Lidwien Speleers, AMOLF, Amsterdam, The Netherlands, for providing the paint cross section HSTB 34/2. The research at AMOLF is embedded in the FOM research program 49 "Mass spectrometric imaging and structural analysis of biomacromolecules". This work is part of the "De Mayerne" program funded by the Dutch Organization for Scientific Research (NWO) and the Foundation for Fundamental Research on Matter (FOM), a subsidiary of the Dutch Organization for Scientific Research (NWO).

SUPPORTING INFORMATION AVAILABLE

Additional information concerning Figure 1: The BSE image visualizes a black particle containing hot spots of smaller than 100 nm. These hot spots are nanoparticles of metallic mercury. This material is available free of charge via the Internet at http://pubs.acs.org.

Received for review December 14, 2004. Accepted April 18, 2005.

AC048158F